Article

Neuron

Balancing the Robustness and Efficiency of Odor Representations during Learning

Highlights

- Learning modifies the robustness and efficiency of odor codes in olfactory bulb
- Learning of difficult discrimination enhances robustness
- Learning of easy discrimination enhances efficiency
- Task learning and passive exposure induce qualitatively similar changes

Authors

Monica W. Chu, Wankun L. Li, Takaki Komiyama

Correspondence

tkomiyama@ucsd.edu

In Brief

Robustness and efficiency are antagonistic factors that affect the effectiveness of sensory codes. Using longitudinal two-photon calcium imaging, Chu et al. (2016) find that learning balances the robustness and efficiency of olfactory bulb odor codes bidirectionally depending on odorant similarity.

Chu et al., 2016, Neuron *92*, 174–186
October 5, 2016
http://dx.doi.org/10.1016/j.neuron.2016.09.004

CellPress

CellPress

Neuron
Article

Balancing the Robustness and Efficiency of Odor Representations during Learning

Monica W. Chu,[1] Wankun L. Li,[1] and Takaki Komiyama[1,2,3,*]
[1]Neurobiology Section, Center for Neural Circuits and Behavior, and Department of Neurosciences
[2]JST, PRESTO
University of California, San Diego, La Jolla, CA 92093, USA
[3]Lead Contact
*Correspondence: tkomiyama@ucsd.edu
http://dx.doi.org/10.1016/j.neuron.2016.09.004

SUMMARY

For reliable stimulus identification, sensory codes have to be robust by including redundancy to combat noise, but redundancy sacrifices coding efficiency. To address how experience affects the balance between the robustness and efficiency of sensory codes, we probed odor representations in the mouse olfactory bulb during learning over a week, using longitudinal two-photon calcium imaging. When mice learned to discriminate between two dissimilar odorants, responses of mitral cell ensembles to the two odorants gradually became less discrete, increasing the efficiency. In contrast, when mice learned to discriminate between two very similar odorants, the initially overlapping representations of the two odorants became progressively decorrelated, enhancing the robustness. Qualitatively similar changes were observed when the same odorants were experienced passively, a condition that would induce implicit perceptual learning. These results suggest that experience adjusts odor representations to balance the robustness and efficiency depending on the similarity of the experienced odorants.

INTRODUCTION

The stimulus space in the environment is infinitely large and continuous. Sensory systems need to effectively represent these stimuli according to perceptual categories, which are often defined through learning. For example, it has been shown that parents of identical twins learn to use subtle visual cues to discriminate between their own twin children, but the effect of this learning is highly specific and does not generalize to other twins (Saether and Laeng, 2008). We consider the effect of learning on two factors related to the effectiveness of sensory representations. First, the representations need to be robust, maintaining a consistent identification of the same stimuli across multiple trials, which can be achieved by encoding redundant information across many channels. Second, representations should be efficient, allowing the encoding of a large number of distinct stimulus categories within the constraint of a finite capacity of sensory systems. We note that efficiency in this sense is not directly related to metabolic costs but instead is a measure of how many distinct stimuli a system can encode. In a system with stable signal-to-noise ratio within individual channels, as well as biological levels of interneuronal correlations, robustness and efficiency are opposing factors that are at odds with each other. For example, if each stimulus is represented by a completely distinct ensemble of neurons, it would be very robust but inefficient, limiting coding capacity (Figure 1A, top). In contrast, if representations of different stimuli are highly overlapping, it would be efficient but sensitive to noise (Figure 1A, bottom). Here we address how these two factors are adjusted during learning in the olfactory system of mice.

Olfactory transduction begins when an odorant binds to odorant receptors on olfactory sensory neurons (OSNs), whose cell bodies lie in the nasal epithelium. Each OSN expresses only one of ~1,000 odorant receptors (Buck and Axel, 1991), and all OSNs expressing a given receptor converge their axons onto one or two glomeruli in the olfactory bulb (Mombaerts et al., 1996). Here the OSN axons synapse onto the dendrites of mitral/tufted cells, the principal neurons of the bulb, each of which projects their dendrites to a single glomerulus and in turn sends out axons to higher areas of the brain. Thus, olfactory information entering higher brain areas from the olfactory bulb is encoded within the activity of mitral/tufted cell ensembles.

The olfactory bulb does not function as a passive relay station from the nose to higher brain areas. Instead, it processes olfactory information owing to the functions of the large population of local interneurons (Arevian et al., 2008; Banerjee et al., 2015; Isaacson and Strowbridge, 1998; Kato et al., 2013; Schoppa et al., 1998; Yokoi et al., 1995). Additionally, feedback from the olfactory cortex and neuromodulatory areas modulates mitral cell odorant responses and is important for olfactory tasks such as odor discrimination and detection (Boyd et al., 2012; Chapuis and Wilson, 2013; Chaudhury et al., 2009; Doucette and Restrepo, 2008; Kapoor et al., 2016; Linster et al., 2001; Ma and Luo, 2012; Otazu et al., 2015). These modulatory functions are sensitive to brain states, as neural activity in the olfactory bulb during the awake state has been shown to be dramatically different from that during the anesthetized state (Blauvelt et al., 2013; Kato et al., 2012; Kollo et al., 2014; Rinberg and Gelperin, 2006). Recent studies in awake behaving animals are

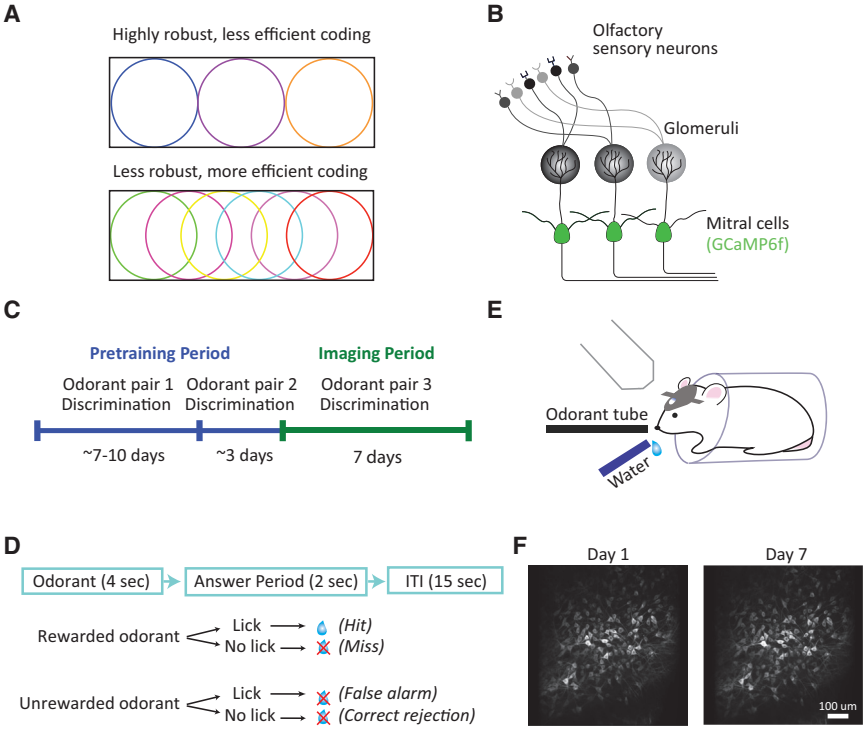

Figure 1. Longitudinal Mitral Cell Imaging during Week-Long Behavioral Paradigms

(A) Schematic demonstrating the tradeoff between robustness and efficiency in the encoding of stimuli within a finite neural activity space (rectangles). (Top) An extreme example of robust coding: three discrete sensory stimuli (colored circles) are encoded with high robustness, or redundancy. (Bottom) An example of a system with higher efficiency, or the capacity to encode more stimuli, than the system above within the same neural space. This enhanced efficiency occurs at the expense of robustness.

(B) Schematic of the olfactory bulb. AAV2.1-FLEX-hsyn-GCaMP6f was injected into the right olfactory bulb of Pcdh21-cre mice to express GCaMP6f specifically in mitral cells.

(C) Experimental timeline. Mice first go through a pre-training period with two sets of odorant pairs (first pre-training pair, citral/limonene; second pre-training pair, +-carvone/cumene) before they started the imaging period, where they perform the discrimination task with a novel odorant pair.

(D) Trial structure of the discrimination task.

(E) Schematic of imaging setup.

(F) A field of mitral cells expressing GCaMP6f on the first day of imaging (left) and 6 days later (right).

beginning to shed light on the way olfactory experience and learning alter the dynamics of olfactory circuits (Abraham et al., 2014; Doucette and Restrepo, 2008; Doucette et al., 2011; Li et al., 2015; Shakhawat et al., 2014). However, a comprehensive understanding of how different types of experience affect odor representations in the early stages of processing is still lacking.

Here we attempt a systematic examination of changes in mitral cell odor representations during four types of week-long odor experience: active learning, where mice perform either an "easy" or "difficult" discrimination task between dissimilar or similar odorant pairs, and passive experience, where mice are passively and repeatedly exposed to the same disimilar or similar pair of odorants as in the behavioral tasks. By using longitudinal two-photon calcium imaging, we monitored the responses of the same populations of mitral cells over a week. Our results indicate that the difficulty level of discrimination has a profound impact on the changes of mitral cell odor representations.

RESULTS

In all conditions, Pcdh21-Cre mice were injected in the right olfactory bulb with Cre-dependent AAV to express GCaMP6f specifically in mitral/tufted cells (Figure 1B). In the discrimination task (Komiyama et al., 2010), one of two odorants was presented in each trial for 4 s, followed by the answer period during which mice were supposed to lick in response to one of the odorants for a water reward and withhold from licking to the other odorant. Mice were trained daily, one session per day, and performed 138.6 ± 1.9 (mean ± SEM) trials per session. Mice first underwent pre-training, which familiarized them with the task with odorant pairs that were different from those used for the imaging experiments (Figures 1C and 1D). After pre-training, mice performed the discrimination task with a novel pair of odorants over 7 days while we imaged the responses of mitral cell ensembles (67 ± 5.4 mitral cells per mouse, mean ± SEM). The same population of mitral cells was imaged in each session (Figures 1E and 1F) (Kato et al., 2012).

Easy Discrimination Training Results in More Efficient Mitral Cell Encoding

We first asked whether and how mitral cell odor representations were altered during a week of discrimination training with a pair of distinct monomolecular odorants (Heptanal, S+ or "odorant 1" and Ethyl Tiglate, S− or "odorant 2"; n = 8 mice). In this easy discrimination task, mice mastered the task within the first tens of trials in the first session and maintained a high success rate on subsequent sessions (Figure 2A).

Each odorant elicited responses from a large fraction of mitral cells on the first day of training. On average, 41.6% ± 7.5% of the imaged mitral cell population exhibited significant changes in fluorescence to at least one odorant during the odor period. The odorant responses included both increases and decreases in fluorescence (day 1, 72.3% ± 9.0% of responses were increases and 27.7% ± 9.0% were decreases; day 7, 72.2% ± 7.0% of responses were increases and 27.8% ± 7.0% were decreases), consistent with previous reports (Bathellier et al., 2008; Davison and Katz, 2007; Doucette and Restrepo, 2008; Fuentes et al., 2008; Gschwend et al., 2012; Kato et al., 2012; Kollo et al.,

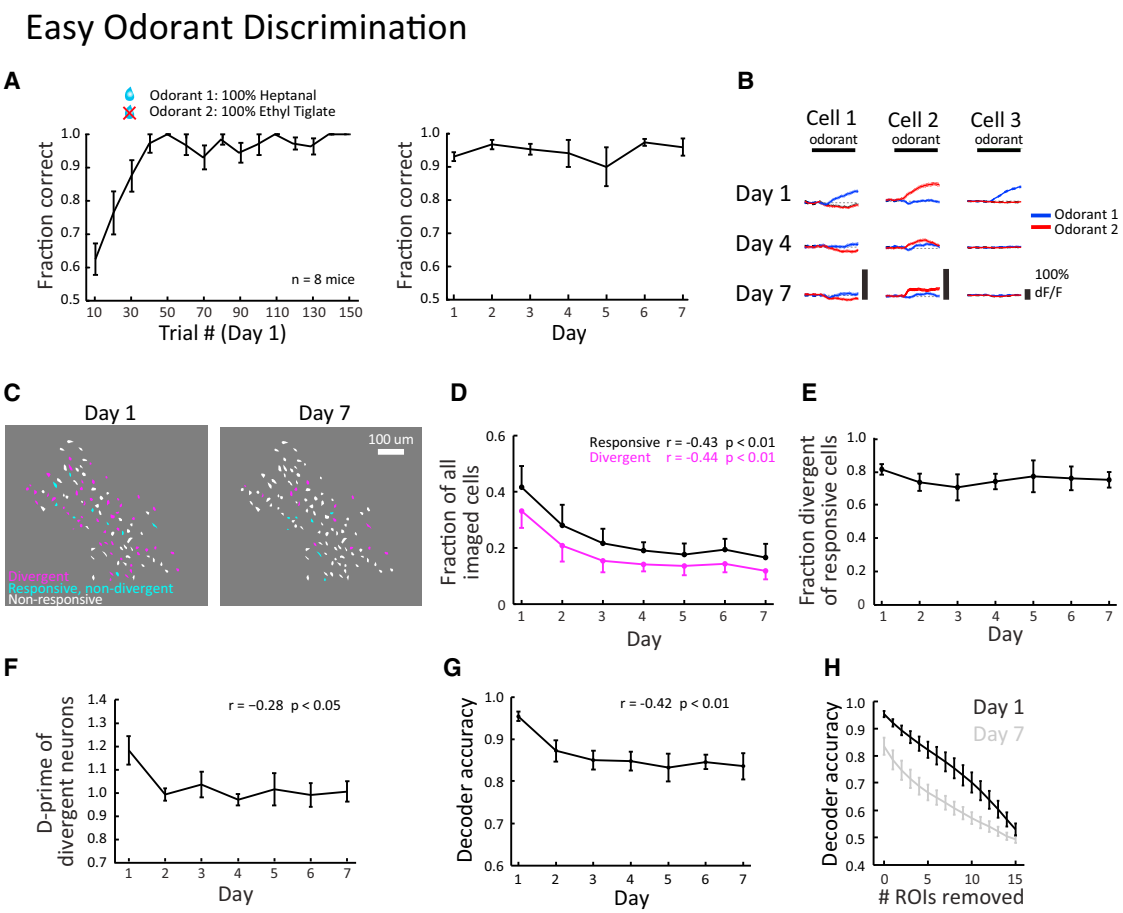

Figure 2. Mitral Cell Odorant Responses during the Easy Discrimination Task

(A) (Left) Behavioral performance on day 1 of the easy discrimination task. Fraction of correct trials is shown for each block of 10 trials (n = 8 mice). (Right) Behavioral performance for each session (day) during the easy discrimination task.

(B) Mean odorant responses of three example mitral cells during single sessions. Horizontal bars indicate odorant periods (4 s).

(C) Spatial distribution of responsive (cyan) and divergent (magenta) neurons on day 1 (left) and day 7 (right) for an example mouse during easy discrimination training. Non-responsive neurons are shown in white.

(D) Fractions of neurons classified as responsive (black) and divergent (magenta) on each day. Both fractions show a significant decrease (Pearson correlation; responsive, $r = -0.43$, $p < 0.01$; divergent, $r = -0.44$, $p < 0.01$).

(E) Fraction of divergent neurons out of responsive neurons is maintained throughout easy discriminating training (Pearson correlation; $r = -0.03$, $p = 0.82$).

(F) Sensitivity index (d′) of divergent neurons decreases with easy discrimination training (Pearson correlation; $r = -0.28$, $p < 0.05$).

(G) Decoder accuracy during easy discrimination training significantly decreases (Pearson correlation; $r = -0.42$, $p < 0.01$)

(H) Coding of odorant identity in mitral cell ensembles is distributed. For each mouse, the mean decoder accuracy was calculated after removing one additional neuron at a time in the descending order of their contribution to decoder accuracy (i.e., the drop in decoder accuracy caused by removal; Experimental Procedures).

All values in line plots are mean ± SEM.

2014; Li et al., 2015; Nagayama et al., 2004; Rinberg and Gelperin, 2006; Shusterman et al., 2011; Yokoi et al., 1995). Additionally, a large fraction of the responsive mitral cells exhibited divergent responses between the two odorants on day 1 (Figures 2B–2D and S1).

During the week-long training paradigm, we observed notable changes in the odorant responses of individual mitral cells. First, there was a gradual decrease in the fraction of responsive mitral cells, from 41.6% ± 7.5% responsive on day 1 to 16.6% ± 4.9% on day 7 (Figure 2D). Both of the two odorants showed a similar level of sparsening during training (Figure S2). Second, the fraction of cells whose responses significantly discriminate the two odorants ("divergent cells") also decreased (from 33.1% ± 6.0% on day 1 to 11.8% ± 3.0% on day 7) (Figure 2D). As a result, the proportion of divergent mitral cells out of the responsive population on each day was maintained (Figure 2E). Next we quantified the discriminability of individual divergent cells using the sensitivity index d′. The average sensitivity index of mitral cells classified as divergent on each day decreased slightly with learning (Figure 2F). Thus, during the learning of the easy discrimination task, information about odorant identity became encoded in fewer mitral cells and less robustly in individual cells.

Difficult Odorant Discrimination

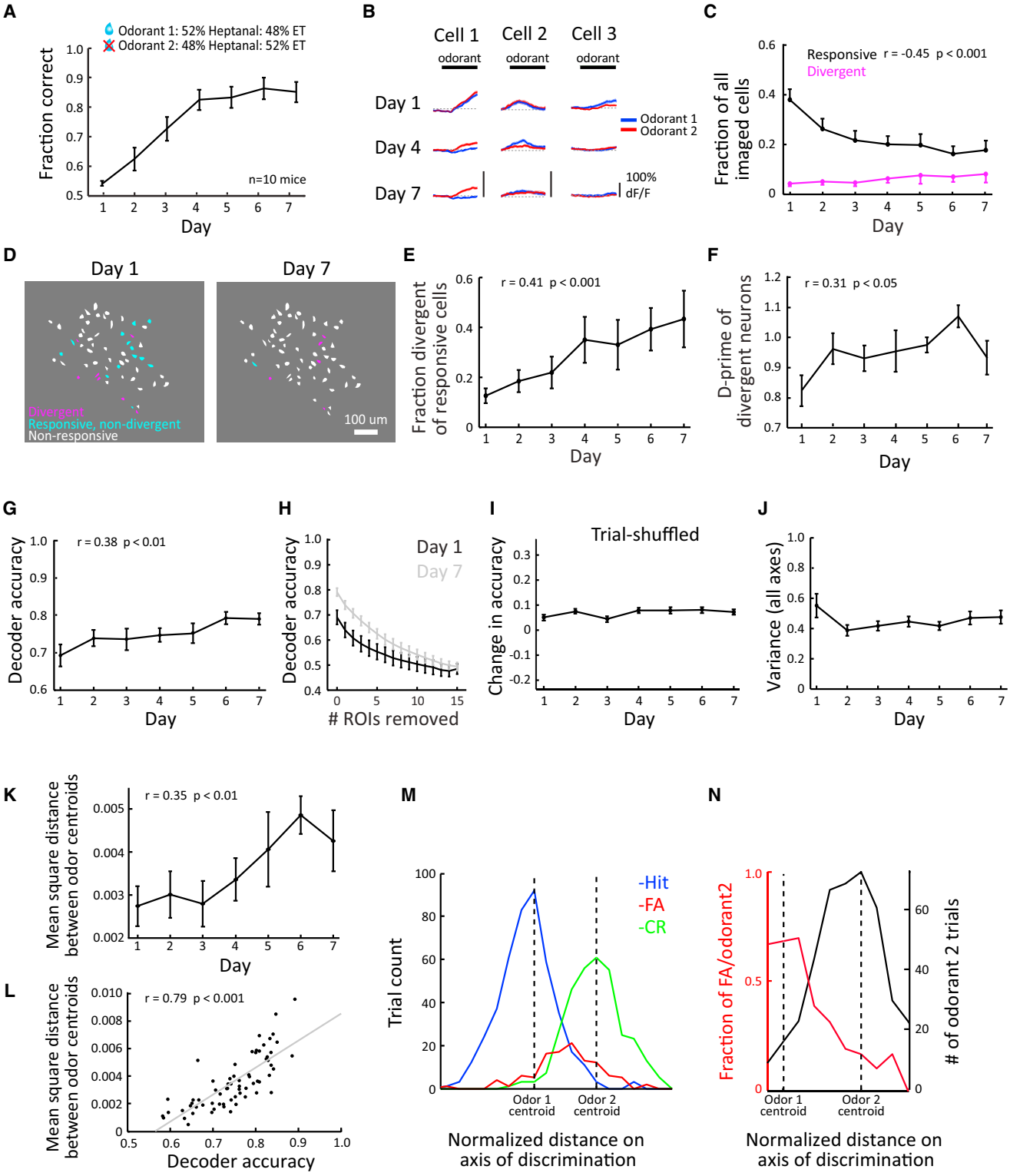

(legend on next page)

Given these changes in mitral cell odorant responses, we next asked whether the quality of encoding of odorant identity by mitral cell populations changed during learning. To this end, we performed a decoder analysis to test how well the representations of the two odorants were separated. Briefly, the population response in each trial was expressed as a high dimensional vector, and we asked whether the vector of a given trial was closer to the centroid of the trials (excluding the trial of interest) of the same odorant (correct classification) or of the other odorant (incorrect classification). We repeated this procedure for every trial and calculated the frequency of correct classification on each day (Experimental Procedures). On the first day, decoder performance was nearly perfect, with an average of 95.4% ± 1.1% correct classifications, reflecting the discrete representations of the two dissimilar odorants (Figure 2G). The decoder performance significantly decreased on subsequent training days, with a mean of 83.6% ± 3.1% correct classifications on day 7. Other methods of decoding, namely linear discriminant analysis (LDA) and support vector machine (SVM), yielded similar results (Figure S3). In contrast, we found that the correlation coefficient, a commonly used measure for the similarity of ensemble activity, was sensitive to the sparsening in our dataset and proved not to be a reliable measure of activity separability (Figure S4). Thus, below we focused on decoder analysis. We note that the imperfect decoder performance after training, which is below the behavioral performance of the mice (Figure 2A), is likely due to the limited number of mitral cells used for the decoder, as mice have access to a much larger population of mitral cells to accurately identify the odorants. Finally, to assess whether the decoder performance relies on a small number of highly divergent mitral cells or uses information distributed across many mitral cells, we calculated how the decoder accuracy degrades as we reduce the number of mitral cells (Experimental Procedures). The decoder accuracy gradually deteriorated as we removed the most informative mitral cell at each permutation, suggesting that the information about odorant identity is highly distributed. This trend was generally maintained throughout training (Figure 2H).

In summary, the easy discrimination task resulted in a gradually smaller separability of the representations of the two dissimilar odorants. We reasoned that this counterintuitive change may be due to the fact that the two odorants were very different. In this case, the discrimination is very easy and thus not the limiting factor of behavioral performance, which may allow the system to reduce the robustness of odor representations and prioritize the efficiency. If so, the difficulty level of discrimination may be an important factor determining the directionality of changes, a notion that we tested in the following section.

Difficult Discrimination Training Results in More Robust Encoding of Odorant Identity

In the difficult discrimination task, a separate cohort of mice (n = 10) were imaged while they were trained with a pair of binary odorant mixtures after the pre-training phase. Odorants were mixed at very similar ratios (odorant 1, 52% heptanal/48% ethyl tiglate; odorant 2, 48% heptanal/52% ethyl tiglate) to ensure the difficulty of discrimination. These ratios were chosen based on results from pilot experiments which tested several ratios in a separate set of mice (data not shown). In contrast to the easy discrimination task, which all mice mastered within the first day, mice demonstrated a slower learning of the difficult discrimination task, suggesting that the similar odorant mixtures were more challenging to discriminate. On the first day, mice had a mean success rate of 53.3% ± 1.0%, indicating that mice were initially unable to distinguish between the odorant mixtures. The performance gradually improved on subsequent days and mice required on average 4 days to perform above an 80% success rate (Figure 3A).

During this week-long training, we observed notable changes in individual mitral cell responses. First, as observed during easy discrimination, there was a sparsening of mitral cell responses,

Figure 3. Mitral Cell Odorant Responses during the Difficult Discrimination Task

(A) Behavioral performance during the difficult discrimination task (n = 10 mice).

(B) Mean odorant responses of three example mitral cells during difficult discrimination training. Horizontal bars indicate odorant periods (4 s).

(C) Fractions of neurons classified as responsive (black) and divergent (magenta) on each day. The responsive fraction shows a significant decrease (Pearson correlation; $r = -0.45$, $p < 0.001$), while the divergent fraction remains stable (Pearson correlation; $r = 0.20$, $p = 0.10$).

(D) Spatial distribution of responsive (cyan) and divergent (magenta) neurons on day 1 (left) and day 7 (right) for an example mouse during difficult discrimination training.

(E) Fraction of divergent neurons out of responsive neurons increases throughout difficult discriminating training (Pearson correlation; $r = 0.41$, $p < 0.001$).

(F) The sensitivity index (d′) of divergent neurons increases with difficult discrimination training (Pearson correlation; $r = 0.31$, $p < 0.05$).

(G) Population decoder accuracy is enhanced during difficult discrimination training (Pearson correlation; $r = 0.38$, $p < 0.01$).

(H) Coding of odorant identity in mitral cell ensembles is distributed.

(I) Improvement in decoder accuracy is not due to changes in interneuronal correlation structure. When each odorant's trial responses were shuffled independently for each cell to eliminate noise correlation, decoder accuracy slightly improved, and this effect did not change with training (Pearson correlation; $r = 0.23$, $p = 0.07$).

(J) The trial-by-trial variance of ensemble activity, calculated as the sum of the covariance matrix of a session's activity vector (Methods), does not change with learning (Pearson correlation; $r = -0.04$, $p = 0.72$).

(K) Mean square distance between odor centroids (Methods) significantly increases with learning (Pearson correlation; $r = 0.35$, $p < 0.01$).

(L) Mean square distance between odor centroids and the decoder accuracy are highly correlated (Pearson correlation; $r = 0.79$, $p < 0.001$).

(M) Distribution of all hit, correct rejection (CR), and false alarm (FA) responses on day 7, projected on the axis connecting the two odor centroids. CR and FA distributions are distinct (bootstrap, $p < 0.001$) and the FA trial distribution lies between hit and CR trials.

(N) Probability of false alarms in all odorant 2 trials is higher when mitral cell responses are more similar to odorant 1 trials on day 7 (Spearman correlation; $r = -0.69$, $p < 0.001$).

All values in line plots are mean ± SEM.

with a decrease from 37.8% ± 4.2% responsive on day 1 to 17.6% ± 3.8% responsive on day 7. However, the fraction of mitral cells with divergent responses remained stable (Figures 3B–3D). As a result, the fraction of divergent mitral cells among those that are responsive increased with learning (Figure 3E). Furthermore, the average discriminability of individual divergent cells increased with learning, indicating that, despite the stable fraction of divergent cells out of all imaged cells, individual divergent cells became more robust in encoding the odorant identity (Figure 3F).

Difficult Discrimination Training Results in Enhanced Discriminability by Mitral Cell Populations

Using the same classification method described earlier, we asked whether there was a change in how well the activity of mitral cell ensembles distinguished odorant identity during the difficult discrimination training. The decoder performance on day 1 was significantly lower than that on day 1 of easy discrimination ($p < 0.001$, Wilcoxon rank-sum test), consistent with the difference in the similarity of odorant pairs. In contrast to the degradation of the decoder performance observed during easy discrimination training, the performance of the decoder improved significantly during difficult discrimination training from 0.69 ± 0.03 on day 1 to 0.79 ± 0.02 on day 7, despite the decrease in the number of mitral cells responding to these odorants (Figure 3G). Similarly to the easy discrimination training, the decoder relied on distributed information from large populations of mitral cells (Figure 3H).

It has been proposed that changes in the trial-to-trial correlation structure, specifically an alteration in the relationship between noise correlation and signal correlation, can affect the discriminability of ensemble activity during perceptual learning (Cohen and Maunsell, 2009; Jeanne et al., 2013). However, we found no evidence of such a change mediating the observed improvement in decoder performance. When we shuffled the trials of individual mitral cells within each odorant's trials to eliminate response covariance across cells (noise correlation), the decoder performance consistently improved, indicating that noise correlation is mildly detrimental to the decoder performance ($p < 0.001$, Wilcoxon signed rank test). This effect did not change with training (Figure 3I). Furthermore, trial-to-trial variability of population responses, another potential contributor to the decoder performance, did not change with training (Figure 3J). Instead, the distance between trial-averaged responses of the two odorants within the population activity space increased gradually (Figure 3K). This is reminiscent of a recent study that found that distance (or "signal"), but not noise, increased in the primary visual cortex during visual perceptual learning (Yan et al., 2014). Consistent with the notion that the distance between odorant responses is the main determinant of decoder accuracy, these two measures exhibited very tight correlation on individual days (Figure 3L). The distance, not the variability or correlation structures, was also the main determinant of decoder accuracy in the easy discrimination task (Figures S3 and S5). Taken together, training with the difficult discrimination task results in an increased separation of the representations of the two similar odorants that are initially overlapping.

Mitral Cell Ensemble Activity Correlates with Behavioral Choice

During the difficult discrimination task, behavioral performance plateaued at ~85% success rate after 4 days. The errors were almost exclusively (97.4%, 530 of 544 error trials on days 4–7) false alarms in which mice licked during no-lick trials. We asked whether these error trials could be predicted by mitral cell odorant responses. To address this question, we projected the population responses of individual trials onto the axis connecting the mean responses of odorant 1 and odorant 2 trials ("discrimination axis"). Strikingly, the distributions of false alarm trials and that of correct rejection trials (correct no-lick in no-lick trials) were significantly different ($p < 0.001$, bootstrap), with the false alarm distribution lying in between the mean responses of odorant 1 and odorant 2 trials (Figure 3M). Accordingly, within odorant 2 trials, there was a monotonic relationship between the location of the population response on a given trial along the discrimination axis and the probability of false alarms, with more "odorant 1-like responses" corresponding to a higher frequency of false alarms ($r = -0.69$, $p < 0.001$, Spearman correlation, Figure 3N). These results suggest that, when mitral cells respond to odorant 2 in an "odorant 1-like" manner, mice are more likely to perceive it as odorant 1.

Population Responses in the Principal Component Space

The results so far suggest that mitral cell odor representations undergo distinct changes in the easy and difficult discrimination tasks. In order to visualize the changes in the high-dimensional mitral cell population responses, we next performed principal component analysis. This allowed us to project odorant responses either for individual mice or for pooled responses across all mice in a space with reduced dimensions. Consistent with the observations with the decoder analysis, in the easy discrimination task, the representations of the two odorants were highly discrete and non-overlapping on day 1. After the training, the representations became closer in the activity space, although they were still relatively distinct (Figures 4A and 4B). In contrast, in the difficult discrimination task, mitral cell odor representations were initially highly overlapping on day 1, reflecting the high similarity of the two odorants. With difficult discrimination training, however, the representations of the two odorants became more separable and discrete by day 7 (Figures 4C and 4D).

Changes in Mitral Cell Responses during Passive Exposure Are Qualitatively Similar to the Task Condition

It has been argued that passive exposure to similar odorants can enhance spontaneous discrimination (Escanilla et al., 2008; Mandairon et al., 2006). We therefore asked whether the changes in mitral cell responses that we observed in behaving mice require engagement in a behavioral task. To address this question, we imaged mitral cell responses (64 ± 4.6 mitral cells per mouse, mean ± SEM) in a separate cohort of mice experiencing odorants passively. In these experiments, two groups of mice were handled identically to the behavioral experiments, including surgeries, water restriction, and pre-training. After pre-training, they experienced the same similar

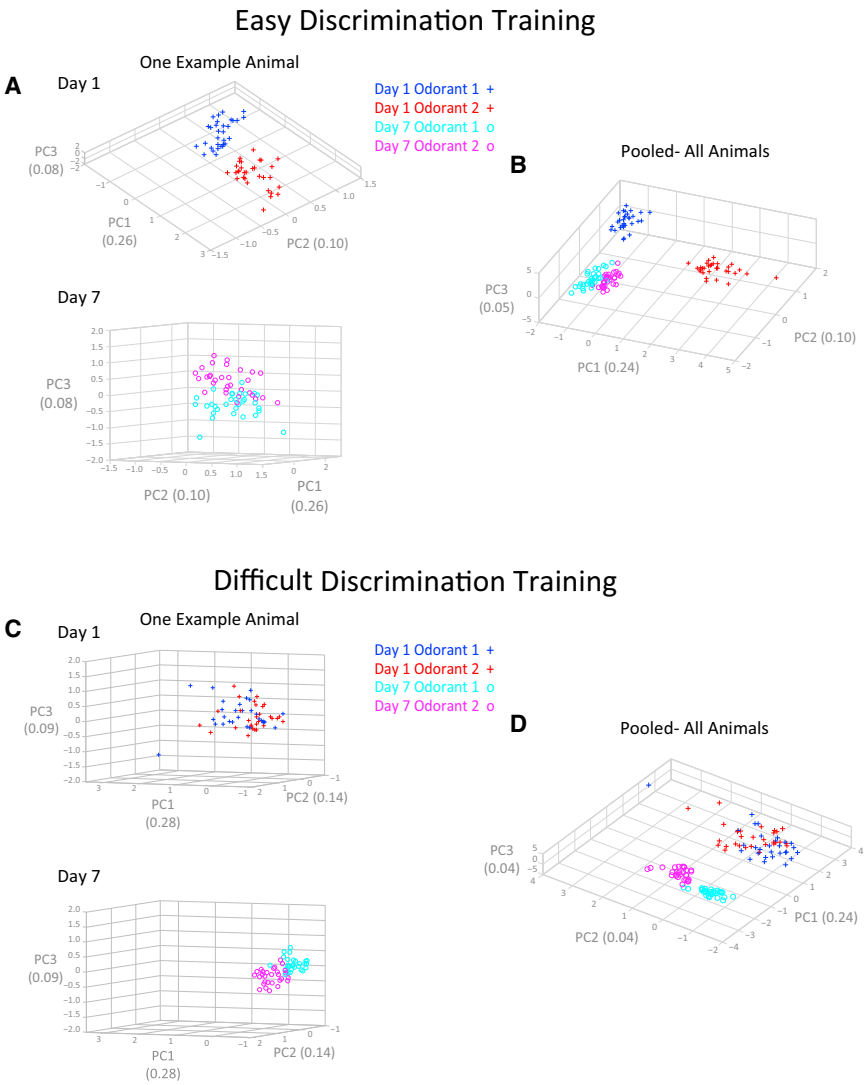

Figure 4. Bidirectional Changes in the Divergence of Population Representations during the Easy and Difficult Discrimination Tasks

(A) Mitral cell population responses from a single mouse in the easy discrimination task visualized in the space of the first three principal components (PC) on day 1 (top) and day 7 (bottom). Each data point corresponds to the population activity on a trial.

(B) Mitral cell population responses pooled across all animals in the easy discrimination task, plotted for day 1 and day 7 in the first three PC axes. Note the decrease in separation of odorant 1 and odorant 2 trials with training.

(C and D) Same as in (A) and (B) for the difficult discrimination task. Note the increase in separation of odorant 1 and odorant 2 trials with training. The value next to each PC axis label is the variance accounted for by that PC axis, and plots are manually rotated to optimally highlight any separability between odorants.

or dissimilar odorant pairs as used in the behavioral tasks at similar time intervals (4 s odorant, 15 s interval, ~75 trials per odorant per day, pseudorandom delivery of the two odorants) passively over 7 days without task engagement (n = 11 mice for difficult odorants and 8 mice for easy odorants). In these conditions, we observed a similar reduction in the fraction of responsive mitral cells as with the task condition (Figures 5A and 5D). Further, the fraction of cells with divergent responses also followed a similar trend as that in task animals, with a stable divergent fraction in animals experiencing similar odorants and a decreasing fraction in animals experiencing dissimilar odorants (Figures 5A, 5B, 5D, and 5E). The decoder performance slightly increased and decreased for similar and dissimilar odorants, respectively, analogous to the case in task animals. However, although the change in decoder accuracy became significantly lower with passive exposure to easy odorants (Figure 5C), it did not reach statistical significance after passive exposure to difficult odorants (Figure 5F). These results suggest that the bidirectional neural changes that we identify in this study are not specific to the association learning condition but instead are a result of becoming familiar with the odorants. Task engagement may either accelerate and/or exaggerate the enhancement or deterioration of discriminability.

DISCUSSION

In this study, we examined the effects of different types of olfactory experience on mitral cell odor representations. Over a week, mice repeatedly experienced a similar or dissimilar odorant pair in a discrimination task or passive exposure. We acknowledge that it is becoming increasingly clear that fine temporal features of mitral cell spiking, which are not accessible with the temporal resolution of our imaging approach, can carry important information about odorant identity (Bathellier et al., 2008; Blauvelt et al., 2013; Blumhagen et al., 2011; Cury and Uchida, 2010; Friedrich et al., 2004; Gschwend et al., 2012; Lepousez and Lledo, 2013; Li et al., 2015; Shusterman et al., 2011). It has also been shown that the reaction time in olfactory discrimination tasks can be as short as a couple hundred milliseconds (Abraham et al., 2004; Resulaj and Rinberg, 2015; Uchida and Mainen, 2003), indicating that mitral cell responses within this time window must contain sufficient information for discrimination at least in certain contexts. While there is certainly value in studying the minimal neural responses necessary for discrimination, our task is not a reaction time task and is not designed to address this problem. We also believe that mitral cell responses within the first couple hundred milliseconds after stimulus onset are unlikely to explain the entirety of our odor percepts, and here we chose to probe the quality of olfactory representations during the entire stimulus period.

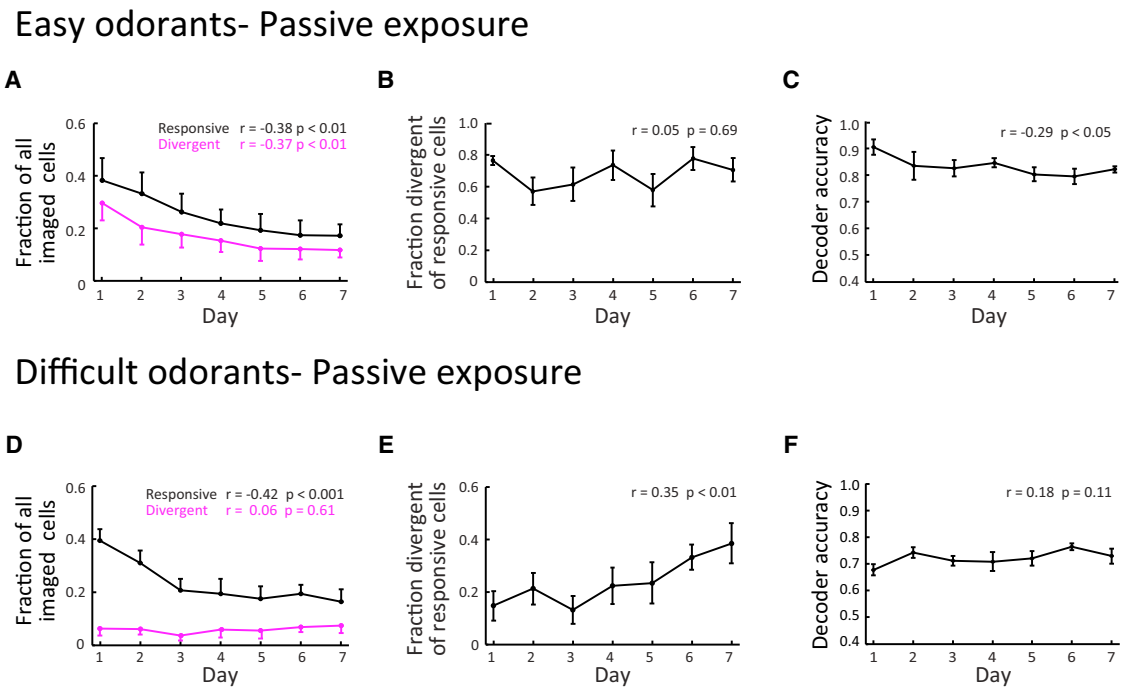

Figure 5. Mitral Cell Odor Responses during Passive Experience

(A–C) Passive experience of the same odorants used in the easy discrimination task (n = 8 mice). (A) Fraction of neurons classified as responsive (black) and divergent (magenta) on each day. There is a significant decrease of both fractions (Pearson correlation; responsive, $r = -0.38$, $p < 0.01$; divergent, $r = -0.37$, $p < 0.01$). (B) Fraction of divergent neurons out of responsive neurons is stable during the week-long passive exposure (Pearson correlation; $r = 0.05$, $p = 0.69$). (C) Decoder accuracy significantly decreases (Pearson correlation; $r = -0.29$, $p < 0.05$).

(D–F) Same as (A)–(C) for passive experience of the same odorants used in the difficult discrimination task (n = 11 mice). (D) Fraction of neurons classified as responsive decreases (Pearson correlation; $r = -0.42$, $p < 0.001$), while the divergent fraction does not change (Pearson correlation, $r = 0.06$, $p = 0.61$). (E) Fraction of divergent neurons out of responsive neurons increases (Pearson correlation; $r = 0.35$, $p < 0.01$). (F) Decoder accuracy is stable (Pearson correlation, $r = 0.18$, $p = 0.11$).

All values in line plots are mean ± SEM.

Regardless, our imaging preparation affords a unique opportunity to perform longitudinal recording from identified mitral cell ensembles across days, allowing a glimpse at the dynamics of odor representations over a week of experience paradigms. We found that all experience paradigms resulted in a sparsening of mitral cell odorant responses. Furthermore, discrimination training significantly modified the discriminability of odorant pairs by mitral cell ensemble responses: discriminability increased with training with similar odorant pairs, mirroring the improvements in the animal's behavioral performance. However, during the discrimination of dissimilar odor pairs, discriminability surprisingly decreased while behavioral performance remained high.

Robustness and Efficiency of Sensory Coding

Information theory articulates the importance of considering the robustness and efficiency of information codes (Shannon, 1948). A reliable code should be robust against many factors that degrade the quality of the code. For example, we have found that the activity of individual mitral cells is variable from trial to trial, making odor representations noisy. Furthermore, we observed that noise correlation among mitral cells has an overall negative impact on the classification of odorant identity. A common way to combat these problems is to increase redundancy, which enhances the robustness of the code. In fact, it has been shown that retinal ganglion cell populations encode the visual scene with a 10-fold redundancy (Puchalla et al., 2005). However, increasing redundancy can come at the expense of the efficiency, decreasing the capacity of distinct information that a sensory system can code. Then how should a sensory system find the right balance between robustness and efficiency? Our results suggest that these factors are dynamically adjusted through learning. This process is context dependent, and the similarity of experienced odorants is an important determinant that governs the direction of the change. When the odorants are very similar, robustness is enhanced at the expense of efficiency. When dissimilar odorants are experienced and the discrimination is easy, the system makes the code more efficient by reducing the robustness, perhaps because it can afford to do so.

A striking feature of our results is that, after easy and difficult discrimination learning, the representations of the two odorants approached a similar level of decorrelation. In other words, the final difference between the representations of the two odorants was nearly independent of how similar the odorants were. This unexpected observation makes it tempting to speculate that

learning balanced the robustness and efficiency of the odor representations to an optimal level. It is important to note that there is not a single optimal value of this balance that applies to all systems. Rather, the optimality is a function of a number of factors including the statistics of sensory inputs and the noise levels of the sensory code. It also depends on the downstream decoding mechanisms. As such, it has been argued that neural circuits should adapt based on these dynamic factors to achieve optimality with learning (Tkacik et al., 2010). We acknowledge that the stimulus set used in our study is not sufficient to test the limit of coding capacity. Future experiments involving a larger number of odorants will be required to better gauge the efficiency in the odorant coding space. Regardless, our results provide empirical evidence that learning can indeed modify the balance between robustness and efficiency in a bidirectional manner.

The Effect of Experience on Olfactory Processing

Previous studies have described learning-related plasticity at multiple levels within the olfactory system (Abraham et al., 2014; Chapuis and Wilson, 2012; Doucette and Restrepo, 2008; Doucette et al., 2011; Kass et al., 2013, 2016; Li et al., 2015; Shakhawat et al., 2014). Our study contributes to the mounting evidence supporting the olfactory bulb as an important locus for learning-related activity changes (Abraham et al., 2014; Doucette and Restrepo, 2008; Doucette et al., 2011; Li et al., 2015). It is noteworthy that one previous study described that olfactory perceptual learning, similar to the difficult discrimination task used here, resulted in increased pattern separation in anterior piriform cortical ensembles but not in mitral cells (Chapuis and Wilson, 2012). One important difference from our current study was that recordings in this study were performed in anesthetized animals. We have previously shown that anesthesia blocked the expression of one form of mitral cell plasticity (Kato et al., 2012), which may explain why their recordings under anesthesia did not reveal the mitral cell plasticity that we report here. A recent study reported that the degree of decorrelation in mitral cell ensemble responses to different odorants before learning could closely predict the difficulty of discrimination learning, although this study did not examine the effect of learning on mitral cell responses (Gschwend et al., 2015). Taking these results together, we suggest that one consequence of difficult discrimination learning is the disambiguation of similar mitral cell odor representations, which could contribute to the improved perceptual acuity during learning. This change at the mitral cell level may occur in concert with additional changes in higher brain areas. Furthermore, this enhanced pattern separation is not observed during easy discrimination learning, in which the odorants already elicit discrete mitral cell odor representations.

We do not believe that many of the changes that we report here are directly related to the association learning aspect of our task. One of our main findings is the bidirectional and opposing changes in discriminability depending on discrimination difficulty, and this finding is not immediately compatible with the notion that the changes are driven by association. Furthermore, neural changes during the passive exposure paradigm were qualitatively similar to the task condition, albeit slightly less pronounced. Therefore it appears that task engagement accelerates and/or exaggerates experience-driven changes whose directionality depends on the similarity of odorants. It is important to note that we should not confuse passive exposure with a learning-free condition. In fact, passive experience has been found to induce implicit perceptual learning in various sensory modalities (Escanilla et al., 2008; Kass et al., 2016; Mandairon et al., 2006; Godde et al., 2000; Watanabe et al., 2001). We propose that a goal of these experience-driven changes in mitral cell responses is to optimally represent the olfactory world based on the statistics of experienced odorant sets.

The changes in mitral cell responses could be mediated by several mechanisms. Local inhibitory neurons within the olfactory bulb, consisting of various subtypes, are likely involved in regulating mitral cell responses in an experience-dependent manner. We previously showed that anesthesia greatly reduces the activity of granule cells, the most abundant inhibitory neurons in the bulb, and blocks the expression of mitral cell sparsening after passive experience (Kato et al., 2012). These results are consistent with the notion that granule cell activity is responsible for the sparsening of mitral cell odor responses. Furthermore, another study reported that an artificial elevation of inhibitory neuron activity in the bulb can enhance pattern separation by mitral cell population responses and improve behavioral performance (Gschwend et al., 2015). An interesting feature about the olfactory bulb is that many inhibitory interneurons are continually replaced with new neurons through adult neurogenesis. It has been reported that recently born neurons are more plastic (Kelsch et al., 2009; Nissant et al., 2009), and artificial activation of these young neurons is particularly effective in enhancing discrimination learning (Alonso et al., 2012). Additionally, the olfactory bulb receives heavy feedback from cortical and neuromodulatory areas. These feedback projections have also been reported to shape mitral cell tuning and influence olfactory perceptual acuity (Doucette et al., 2007; Ma and Luo, 2012; Otazu et al., 2015; Rothermel et al., 2014). Future studies will be needed to unravel the relative contributions of these related mechanisms to the mitral cell plasticity induced by different types of odor experience.

EXPERIMENTAL PROCEDURES

Subjects

All procedures were in accordance with protocols approved by the UCSD Institutional Animal Care and Use Committee and guidelines of the National Institute of Health. Mice (Pcdh21-Cre) were originally acquired from RIKEN BRC and backcrossed at least four times to C57bl/6. Mice were housed in disposable plastic cages with standard bedding in a room with a reversed light cycle (12 hr/12 hr), and all experiments were performed during the dark period.

Surgeries

Adult mice (6 weeks or older, male) were anesthetized with isoflurane, and surgeries were performed to implant a headplate and perform craniotomy as described previously (Kato et al., 2012). Briefly, a stainless steel headplate was glued to the skull, followed by the implantation of an optical glass window (1 × 2 mm oval) above the right olfactory bulb and securement with dental cement. To obtain mitral cell-specific expression of GCaMP6f, virus containing a Cre-dependent GCaMP6f-expression construct (AAV2.1 hsyn-FLEX-GCaMP6f, UPenn Vector Core, 1:4 dilution in saline, 20 nl per site, four sites) was injected into the olfactory bulb of Pcdh21-cre mice at the depth of 250 μm during craniotomy.

Odorant Delivery

Odorants were first diluted in mineral oil to a calculated vapor pressure of 200 ppm. A custom-built olfactometer mixed saturated odorant vapor 1:1 with filtered, humidified air for a final concentration of 100 ppm. Final air flow rate was controlled at 1 L/min.

Behavior

Mice were water restricted starting ~1 week after surgeries, and weight was maintained at 80%–85% of initial value. The pre-training phase started 2 weeks after water restriction. The behavioral program was controlled by a real-time system (C. Brody, personal communication). Each daily training session consisted of 150 trials, and odorants were delivered pseudo-randomly with no more than three successive trials of the same odorant. Each trial included an odorant delivery time of 4 s. This was followed by a 2 s answer period where the mouse had the opportunity to respond. If the odorant was the rewarded odorant (S+) and the mouse licked the lickport at least once during the answer period, a water reward is given (~6–7 μl). Any other action (i.e., not licking to S+ or unrewarded odorant [S−], or licking to S−) did not result in a water reward, and the trial would then proceed to the inter-trial interval (ITI). No punishment was delivered for error trials. Licking during the odorant period was ignored.

During the pre-training phase, mice were first trained with a single odorant pair, citral (S+) and limonene (S−), with an ITI of 3 s. After mice performed above 80% success rate, the ITI was incrementally extended by 2 s every half-session until an ITI of 15 s was reached. Once the mice performed at a success rate above 80% for the first odorant pair with an ITI of 15 s (~7–10 days), odorants were changed to a second pair, +-carvone (S+) and cumene (S-). Once mice performed above 80% for the second odorant pair (~3–4 days) and mitral cells expressed GCaMP6f at levels sufficient for imaging, we began the week-long imaging period, where mitral cell activity was monitored while mice simultaneously performed a discrimination task with a novel odorant pair or experienced the novel odorants passively. For passive odorant experience, the trial structure, including odorant delivery time (4 s) and ITI (15 s), was the same as during discrimination training, with the exception that no water reward was given. Licking during passive exposure was rare, decreasing from 6.3% ± 2.5% and 5.2% ± 1.5% of trials on day 1 for easy and difficult odorants, respectively, to 1.9% ± 0.6% and 1.4% ± 0.6% of trials on day 7. The odorants used for the imaging experiments, heptanal and ethyl tiglate, were chosen on the basis of their structural dissimilarity.

Image Acquisition

Two-photon imaging was done with a commercial microscope (B-scope, Thorlabs) with 925 nm excitation from a Ti-Sa laser (Spectra-physics) at a framerate of approximately 28 Hz. Each imaging frame was made up of 512 × 512 pixels, spanning 765 × 655 μm. Imaging was performed continuously during segments of about 2.4 min long, with inter-segment intervals of 7 s. Data from trials which occurred during the intervals were not analyzed. Full-frame cross-correlation correction on imaging frames was performed using a custom program written in MATLAB.

Data Analysis

In a small number of sessions we were not able to collect imaging data due to error, and these sessions were excluded from analysis. These excluded sessions were as follows: difficult odorant discrimination—day 6 (one mouse) and day 7 (two mice); difficult odorants, passive exposure—day 3 (one mouse); easy odorant discrimination—day 7 (two mice). Unless otherwise stated, all values are reported as mean ± SEM.

Determining ROIs

Regions of interest (ROIs) were manually drawn around mitral cells by using a custom MATLAB program on the average image of the first session. For each ROI, a background ROI was also manually drawn in a nearby area that was unoccupied by other labeled cells or neurites. For each subsequent day, each ROI was manually moved to accommodate small shifts, and if any ROI was not visible in any of the imaging days, that ROI was excluded. Pixels values within each ROI were averaged to create fluorescence time series, and values from the corresponding background ROI were subtracted. For each trial for each mitral cell, the time series was normalized to the average fluorescence value during the baseline period (5 s period before odorant onset) to calculate dF/F. The total numbers of cells and animals imaged for each condition are as follows: 731 cells and 10 mice (difficult discrimination training); 736 cells and 11 mice (difficult odors, passive exposure), 467 cells and 8 mice (easy discrimination training), and 479 cells and 8 mice (easy odors, passive exposure).

Classifying Responsive and Divergent Mitral Cells

Responsive and divergent mitral cells were identified in each session using trial traces smoothed with the MATLAB "smooth" function with the time constant of six frames (~0.25 s).

A mitral cell was classified as divergent if both of the following two criteria were met. For criterion 1, dF/F is significantly different ($p < 0.05$) between odorant 1 and odorant 2 trials in at least 75% of the time points within any 0.5 s window during the odorant period. p value for each time point was calculated by Wilcoxon rank sum test between dF/F values for odorant 1 and odorant 2 trials. For criterion 2, the difference between trial-averaged dF/F of odorant 1 and odorant 2 trials exceeds 0.225 in at least one time point during the 0.5 s window that meets the first criterion.

A mitral cell was classified as responsive to a given odorant in a given session if one of the following two criteria were met. For criterion 1, the cell is classified as divergent as above. For criterion 2, both of the following criteria are met: (1) dF/F is significantly different ($p < 0.05$) from baseline in at least 75% of the time points (i.e., image frames) within any 0.5 s window during the odorant period. p value for each time point was calculated by Wilcoxon rank sum test between dF/F at that time point from all trials of a given odorant and dF/F of all baseline frames from all trials. (2) The difference between trial-averaged and time-averaged baseline dF/F and trial-averaged dF/F of a given time point exceeds 0.20 in at least one time frame during the 0.5 s window that meets the first criterion.

Based on these classification methods, the false discovery rate calculated by comparisons with shuffled data (Komiyama et al., 2010) was 0% for the criterion 2 of responsive classification (0/2,704,800 cell-odorant-session pairs, calculated by shuffling time points within trials) and 0.33% for divergent classification (420/1,352,400 cell-session pairs, calculated by shuffling trial labels).

Calculating d′ for Divergent Neurons

On each day, the sensitivity index, or d′ (Macmillan and Creelman, 2005), for divergent neurons for each mouse was calculated. First, all trial traces were smoothed with the MATLAB "smooth" function with the time constant of six frames (~0.25 s). If a cell was divergent on a given day, d′ was calculated for each time frame during the odorant period (0–4 s after odorant onset).

$$d' = \frac{\left| mean\frac{dF}{F}_{odorant1} - mean\frac{dF}{F}_{odorant2} \right|}{pooled\ standard\ deviation_{odorant1\ and\ 2}}$$

Then each divergent neuron was assigned the maximum d′ value of all frames during the odorant period, and the average of these maximum d′ values of divergent neurons for each mouse on each session was calculated and plotted in Figures 2F and 3F.

Decoder Analysis

For each mouse, decoder analysis was performed on 100 iterations. In each iteration, 16 mitral cells used for the decoder were randomly drawn from a pool of all mitral cells that were classified as responsive in at least one session. The population size of n = 16 cells was determined by the mouse with the lowest number of responsive mitral cells.

Nearest-Centroid Decoder

For the nearest-centroid classifier (Kato et al., 2012), the mitral cell population response in each trial was expressed as an activity vector, which was a concatenation of the time-averaged dF/F from the first and second 2 s windows during the 4 s odorant period of each mitral cell (16 neurons × 2 values per neuron = 32 dimensional vector). For each trial, centroids for odorant 1 and odorant 2 trials were calculated from all trial activity vectors excluding the trial being scored. The decoder assigned the trial in question the identity of the odorant with the closest centroid. For each iteration, the accuracy of the decoder was calculated as the prediction success rate of the decoder for all trials on each day. For each mouse, the daily accuracy was calculated by taking the average of the 100 iterations.

We next assessed the contributions of individual variables to decoder accuracy. For each iteration, the distance between odor centroids was assessed by first calculating odor centroids, which are the population vectors created from

the mean of all trial activity vectors belonging to each odorant in a session. Then the mean square distance was calculated as the square of the Euclidean distance between odor centroids, divided by the number of neurons in the activity vector. For each mouse, the daily mean square distance was calculated by averaging across 100 iterations.

The trial-to-trial variability for each odorant was assessed by calculating the total variance on each day. For each iteration, the total variance for each odorant on each day was calculated by summing the diagonal of the covariance matrix (summing the variance across each dimension of the activity vector). Mean daily total variance for each mouse and odorant was calculated by averaging across 100 iterations.

The contributions of interneuronal correlations were assessed by disrupting noise correlations through the shuffling of trial responses independently for each neuron. Decoder accuracy was recalculated using activity vectors reconstructed from these shuffled responses for 100 iterations of shuffling. The change in decoder accuracy after disrupting noise correlation was calculated for each mouse in each session by subtracting the original decoder accuracy (without shuffling) from the decoder accuracy after shuffling. Wilcoxon signed rank test was performed, for each condition, on the dataset of concatenated mouse-day pairs of decoder accuracy values for before and after trial shuffling.

To assess how distributed odorant identity information is across mitral cells, the decoder analysis was repeated after removing subsets of 16 neurons. Decoder accuracy was calculated after removing one additional neuron in each iteration in the descending order of their contribution to decoder accuracy (i.e., the drop in decoder accuracy after removal). One hundred iterations were performed for each mouse, where different 16-neuron populations were resampled for each iteration. Average scores were calculated for each mouse by averaging across iterations.

Linear Discriminant Analysis

For the linear discriminant analysis (LDA)-based classifier, the mitral cell population response in each trial used the same trial activity vectors as in the nearest-centroid decoder (see above). The linear classification was performed using the MATLAB function *classify*. For each day, the classifier went through each trial as the test set, using the other remaining trials as the training set. The accuracy of the decoder was calculated as the prediction success rate of the decoder for all trials on each day. For each mouse, the daily accuracy was calculated by taking the average score of the 100 iterations of randomly selected subsets of 16 cells.

The contributions of interneuronal correlations for LDA were assessed in the same way as in nearest-centroid decoder, by the shuffling of trial responses independently for each neuron. The change in decoder accuracy after disrupting noise correlation was calculated for each mouse in each session by subtracting the original decoder accuracy (without shuffling) from the decoder accuracy after 100 iterations of shuffling.

Support Vector Machine

For the support vector machine (SVM)-based classifier, the mitral cell population response in each trial used the same trial activity vectors as in the nearest-centroid classifier (see above). The classification was performed using the MATLAB's *svmtrain* function. The classifier went through each single trial as the test set, using the other remaining trials as the training dataset. The accuracy of the decoder was calculated as the prediction success rate of the decoder for all trials on each day. For each mouse, the daily accuracy was calculated by taking the average of the 100 iterations of randomly selected subsets of 16 cells.

The contributions of interneuronal correlations for SVM were assessed in the same way as in nearest-centroid decoder, with ten iterations of shuffling.

Principal Component Analysis

For individual mice, principal component analysis was performed on a matrix made by concatenating all trial response vectors (defined as above, using all mitral cells that are classified as responsive in at least one session) from day 1 and day 7. For pooling across mice, a matrix of trial response vectors was created for each mouse using the first n trials. A pooled response vector was then created by concatenating across animals. The number of trials n, determined by the session with the lowest number of trials for a single odorant, was 31 for easy discrimination and 29 for difficult discrimination.

Calculating Correlation Coefficients

To calculate correlation coefficients for each day, a mitral cell population response vector was constructed for each trial by concatenating the time-averaged dF/F from the first and second 2 s windows during the 4 s odorant period of each mitral cell. Correlation coefficient between response vectors for each pair of trials was calculated using the MATLAB function *corrcoef*. Averages of trial pairs from two different odorants and same odorants were used as the inter-odorant and intra-odorant correlation coefficient for each mouse, respectively.

SUPPLEMENTAL INFORMATION

Supplemental Information includes five figures and can be found with this article at http://dx.doi.org/10.1016/j.neuron.2016.09.004.

AUTHOR CONTRIBUTIONS

Conceptualization, T.K. and M.W.C.; Methodology, M.W.C. and T.K.; Formal Analysis, M.W.C., W.L.L. and T.K.; Investigation, M.W.C., W.L.L and T.K.; Writing – Original Draft, M.W.C. and T.K.; Writing – Review & Editing, M.W.C., W.L.L. and T.K.; Supervision, T.K.; Funding Acquisition, T.K.

ACKNOWLEDGMENTS

We thank A.N. Kim, K. O'Neil, and L. Hall for technical assistance; A. Mitani for the motion correction program; and L.F. Abbott, A. Fink, I. Imayoshi, C. Schoonover, C.F. Stevens, J. Wang, and members of the Komiyama lab for discussions. This research was supported by grants from NIH (R01 DC014690-01, R21 DC012641, R01 NS091010A, U01 NS094342, and R01 EY025349), Human Frontier Science Program, Japan Science and Technology Agency (PRESTO), New York Stem Cell Foundation, David & Lucile Packard Foundation, Pew Charitable Trusts, and McKnight Foundation (to T.K.) and by NIH Training Grant (5T32GM007240) (to M.W.C.). T.K. is a NYSCF-Robertson Investigator.

Received: April 14, 2016
Revised: July 12, 2016
Accepted: August 23, 2016
Published: September 22, 2016

REFERENCES

Abraham, N.M., Spors, H., Carleton, A., Margrie, T.W., Kuner, T., and Schaefer, A.T. (2004). Maintaining accuracy at the expense of speed: stimulus similarity defines odor discrimination time in mice. Neuron *44*, 865–876.

Abraham, N.M., Vincis, R., Lagier, S., Rodriguez, I., and Carleton, A. (2014). Long term functional plasticity of sensory inputs mediated by olfactory learning. eLife *3*, e02109.

Alonso, M., Lepousez, G., Sebastien, W., Bardy, C., Gabellec, M.-M., Torquet, N., and Lledo, P.-M. (2012). Activation of adult-born neurons facilitates learning and memory. Nat. Neurosci. *15*, 897–904.

Arevian, A.C., Kapoor, V., and Urban, N.N. (2008). Activity-dependent gating of lateral inhibition in the mouse olfactory bulb. Nat. Neurosci. *11*, 80–87.

Banerjee, A., Marbach, F., Anselmi, F., Koh, M.S., Davis, M.B., Garcia da Silva, P., Delevich, K., Oyibo, H.K., Gupta, P., Li, B., and Albeanu, D.F. (2015). An interglomerular circuit gates glomerular output and implements gain control in the mouse olfactory bulb. Neuron *87*, 193–207.

Bathellier, B., Buhl, D.L., Accolla, R., and Carleton, A. (2008). Dynamic ensemble odor coding in the mammalian olfactory bulb: sensory information at different timescales. Neuron *57*, 586–598.

Blauvelt, D.G., Sato, T.F., Wienisch, M., Knöpfel, T., and Murthy, V.N. (2013). Distinct spatiotemporal activity in principal neurons of the mouse olfactory bulb in anesthetized and awake states. Front. Neural Circuits *7*, 46.

Blumhagen, F., Zhu, P., Shum, J., Schärer, Y.-P.Z., Yaksi, E., Deisseroth, K., and Friedrich, R.W. (2011). Neuronal filtering of multiplexed odour representations. Nature *479*, 493–498.

Boyd, A.M., Sturgill, J.F., Poo, C., and Isaacson, J.S. (2012). Cortical feedback control of olfactory bulb circuits. Neuron *76*, 1161–1174.

Buck, L., and Axel, R. (1991). A novel multigene family may encode odorant receptors: a molecular basis for odor recognition. Cell *65*, 175–187.

Chapuis, J., and Wilson, D.A. (2012). Bidirectional plasticity of cortical pattern recognition and behavioral sensory acuity. Nat. Neurosci. *15*, 155–161.

Chapuis, J., and Wilson, D.A. (2013). Cholinergic modulation of olfactory pattern separation. Neurosci. Lett. *545*, 50–53.

Chaudhury, D., Escanilla, O., and Linster, C. (2009). Bulbar acetylcholine enhances neural and perceptual odor discrimination. J. Neurosci. *29*, 52–60.

Cohen, M.R., and Maunsell, J.H. (2009). Attention improves performance primarily by reducing interneuronal correlations. Nat. Neurosci. *12*, 1594–1600.

Cury, K.M., and Uchida, N. (2010). Robust odor coding via inhalation-coupled transient activity in the mammalian olfactory bulb. Neuron *68*, 570–585.

Davison, I.G., and Katz, L.C. (2007). Sparse and selective odor coding by mitral/tufted neurons in the main olfactory bulb. J. Neurosci. *27*, 2091–2101.

Doucette, W., and Restrepo, D. (2008). Profound context-dependent plasticity of mitral cell responses in olfactory bulb. PLoS Biol. *6*, e258.

Doucette, W., Milder, J., and Restrepo, D. (2007). Adrenergic modulation of olfactory bulb circuitry affects odor discrimination. Learn. Mem. *14*, 539–547.

Doucette, W., Gire, D.H., Whitesell, J., Carmean, V., Lucero, M.T., and Restrepo, D. (2011). Associative cortex features in the first olfactory brain relay station. Neuron *69*, 1176–1187.

Escanilla, O., Mandairon, N., and Linster, C. (2008). Odor-reward learning and enrichment have similar effects on odor perception. Physiol. Behav. *94*, 621–626.

Friedrich, R.W., Habermann, C.J., and Laurent, G. (2004). Multiplexing using synchrony in the zebrafish olfactory bulb. Nat. Neurosci. *7*, 862–871.

Fuentes, R.A., Aguilar, M.I., Aylwin, M.L., and Maldonado, P.E. (2008). Neuronal activity of mitral-tufted cells in awake rats during passive and active odorant stimulation. J. Neurophysiol. *100*, 422–430.

Godde, B., Stauffenberg, B., Spengler, F., and Dinse, H.R. (2000). Tactile coactivation-induced changes in spatial discrimination performance. J. Neurosci. *20*, 1597–1604.

Gschwend, O., Beroud, J., and Carleton, A. (2012). Encoding odorant identity by spiking packets of rate-invariant neurons in awake mice. PLoS ONE *7*, e30155.

Gschwend, O., Abraham, N.M., Lagier, S., Begnaud, F., Rodriguez, I., and Carleton, A. (2015). Neuronal pattern separation in the olfactory bulb improves odor discrimination learning. Nat. Neurosci. *18*, 1474–1482.

Isaacson, J.S., and Strowbridge, B.W. (1998). Olfactory reciprocal synapses: dendritic signaling in the CNS. Neuron *20*, 749–761.

Jeanne, J.M., Sharpee, T.O., and Gentner, T.Q. (2013). Associative learning enhances population coding by inverting interneuronal correlation patterns. Neuron *78*, 352–363.

Kapoor, V., Provost, A.C., Agarwal, P., and Murthy, V.N. (2016). Activation of raphe nuclei triggers rapid and distinct effects on parallel olfactory bulb output channels. Nat. Neurosci. *19*, 271–282.

Kass, M.D., Rosenthal, M.C., Pottackal, J., and McGann, J.P. (2013). Fear learning enhances neural responses to threat-predictive sensory stimuli. Science *342*, 1389–1392.

Kass, M.D., Guang, S.A., Moberly, A.H., and McGann, J.P. (2016). Changes in olfactory sensory neuron physiology and olfactory perceptual learning after odorant exposure in adult mice. Chem. Senses *41*, 123–133.

Kato, H.K., Chu, M.W., Isaacson, J.S., and Komiyama, T. (2012). Dynamic sensory representations in the olfactory bulb: modulation by wakefulness and experience. Neuron *76*, 962–975.

Kato, H.K., Gillet, S.N., Peters, A.J., Isaacson, J.S., and Komiyama, T. (2013). Parvalbumin-expressing interneurons linearly control olfactory bulb output. Neuron *80*, 1218–1231.

Kelsch, W., Lin, C.W., Mosley, C.P., and Lois, C. (2009). A critical period for activity-dependent synaptic development during olfactory bulb adult neurogenesis. J. Neurosci. *29*, 11852–11858.

Kollo, M., Schmaltz, A., Abdelhamid, M., Fukunaga, I., and Schaefer, A.T. (2014). 'Silent' mitral cells dominate odor responses in the olfactory bulb of awake mice. Nat. Neurosci. *17*, 1313–1315.

Komiyama, T., Sato, T.R., O'Connor, D.H., Zhang, Y.-X., Huber, D., Hooks, B.M., Gabitto, M., and Svoboda, K. (2010). Learning-related fine-scale specificity imaged in motor cortex circuits of behaving mice. Nature *464*, 1182–1186.

Lepousez, G., and Lledo, P.M. (2013). Odor discrimination requires proper olfactory fast oscillations in awake mice. Neuron *80*, 1010–1024.

Li, A., Gire, D.H., and Restrepo, D. (2015). ϒ spike-field coherence in a population of olfactory bulb neurons differentiates between odors irrespective of associated outcome. J. Neurosci. *35*, 5808–5822.

Linster, C., Garcia, P.A., Hasselmo, M.E., and Baxter, M.G. (2001). Selective loss of cholinergic neurons projecting to the olfactory system increases perceptual generalization between similar, but not dissimilar, odorants. Behav. Neurosci. *115*, 826–833.

Ma, M., and Luo, M. (2012). Optogenetic activation of basal forebrain cholinergic neurons modulates neuronal excitability and sensory responses in the main olfactory bulb. J. Neurosci. *32*, 10105–10116.

Macmillan, N.A., and Creelman, C.D. (2005). Detection Theory: A User's Guide (Mahwah, N.J.: Psychology Press).

Mandairon, N., Stack, C., Kiselycznyk, C., and Linster, C. (2006). Enrichment to odors improves olfactory discrimination in adult rats. Behav. Neurosci. *120*, 173–179.

Mombaerts, P., Wang, F., Dulac, C., Chao, S.K., Nemes, A., Mendelsohn, M., Edmondson, J., and Axel, R. (1996). Visualizing an olfactory sensory map. Cell *87*, 675–686.

Nagayama, S., Takahashi, Y.K., Yoshihara, Y., and Mori, K. (2004). Mitral and tufted cells differ in the decoding manner of odor maps in the rat olfactory bulb. J. Neurophysiol. *91*, 2532–2540.

Nissant, A., Bardy, C., Katagiri, H., Murray, K., and Lledo, P.-M. (2009). Adult neurogenesis promotes synaptic plasticity in the olfactory bulb. Nat. Neurosci. *12*, 728–730.

Otazu, G.H., Chae, H., Davis, M.B., and Albeanu, D.F. (2015). Cortical feedback decorrelates olfactory bulb output in awake mice. Neuron *86*, 1461–1477.

Puchalla, J.L., Schneidman, E., Harris, R.A., and Berry, M.J. (2005). Redundancy in the population code of the retina. Neuron *46*, 493–504.

Resulaj, A., and Rinberg, D. (2015). Novel Behavioral Paradigm Reveals Lower Temporal Limits on Mouse Olfactory Decisions. J. Neurosci. *35*, 11667–11673.

Rinberg, D., and Gelperin, A. (2006). Olfactory neuronal dynamics in behaving animals. Semin. Cell Dev. Biol. *17*, 454–461.

Rothermel, M., Carey, R.M., Puche, A., Shipley, M.T., and Wachowiak, M. (2014). Cholinergic inputs from Basal forebrain add an excitatory bias to odor coding in the olfactory bulb. J. Neurosci. *34*, 4654–4664.

Saether, L., and Laeng, B. (2008). On facial expertise: processing strategies of twins' parents. Perception *37*, 1227–1240.

Schoppa, N.E., Kinzie, J.M., Sahara, Y., Segerson, T.P., and Westbrook, G.L. (1998). Dendrodendritic inhibition in the olfactory bulb is driven by NMDA receptors. J. Neurosci. *18*, 6790–6802.

Shakhawat, A.M., Harley, C.W., and Yuan, Q. (2014). Arc visualization of odor objects reveals experience-dependent ensemble sharpening, separation, and merging in anterior piriform cortex in adult rat. J. Neurosci. *34*, 10206–10210.

Shannon, C.E. (1948). A mathematical theory of communication. Bell Syst. Tech. J. *27*, 379–423.

Shusterman, R., Smear, M.C., Koulakov, A.A., and Rinberg, D. (2011). Precise olfactory responses tile the sniff cycle. Nat. Neurosci. *14*, 1039–1044.

Tkacik, G., Prentice, J.S., Balasubramanian, V., and Schneidman, E. (2010). Optimal population coding by noisy spiking neurons. Proc. Natl. Acad. Sci. USA *107*, 14419–14424.

Uchida, N., and Mainen, Z.F. (2003). Speed and accuracy of olfactory discrimination in the rat. Nat. Neurosci. *6*, 1224–1229.

Watanabe, T., Náñez, J.E., and Sasaki, Y. (2001). Perceptual learning without perception. Nature *413*, 844–848.

Yan, Y., Rasch, M.J., Chen, M., Xiang, X., Huang, M., Wu, S., and Li, W. (2014). Perceptual training continuously refines neuronal population codes in primary visual cortex. Nat. Neurosci. *17*, 1380–1387.

Yokoi, M., Mori, K., and Nakanishi, S. (1995). Refinement of odor molecule tuning by dendrodendritic synaptic inhibition in the olfactory bulb. Proc. Natl. Acad. Sci. USA *92*, 3371–3375.